Application of Genetic Algorithm to Determine Thermal Properties of Microelectronic Layered Structures

Robert Arsoba[1], Zbigniew Suszyński[1]
[1] Koszalin University of Technology,
Department of Electronics and Computer Science,
ul. Śniadeckich 2, 75-453 Koszalin, Poland

Abstract. In the paper, possibilities of application of genetic algorithms to determine thermal properties depth profile in microelectronic layered structures were presented. A developed computational method was described and results obtained using the method for a thyristor structure were presented.

Keywords. Genetic algorithm, inverse problem, microelectronics, thermal properties, layered structure

1 Introduction

Thermal methods belong to the most important methods of non-destructive investigation and testing (NDT). These methods are widely used for detection of internal defects and to determine thermal properties of objects. One of the applications of thermal methods in microelectronics is examination of quality of thermocompression in layered structures. Silicon-aluminium-molybdenum structures used in manufacturing of high power thyristors are an example of such objects.

One of the most interesting challenges in the area of thermal investigations is determination of thermal properties depth profile. Such a problem consists in determination of thermal properties of an examined object basing on measurement results of a temperature response for known energetic excitation (so called *inverse problem*). The inverse problem is a multi-parametric global optimisation task. This task consists in searching for parameters of a thermal model, which are in the best agreement with parameters of an examined object. Even in the case of a one-dimensional modelling, thermal models of examined objects are relatively complex and they are described using functions of many variables. In such a case, classical methods of optimisation (analytical and numerical ones) are ineffective. Therefore, it is advisable to use computing techniques based on artificial intelligence methods.

A review of achievements in the area of solving the inverse problem leads to a conclusion, that nowadays there is no any effective, commonly acknowledged and used method of thermal properties depth profiling in layered structures. Proposed methods are the following: a Fourier analysis [1], a TWBS method (*thermal wave back scattering*) [2], methods based on artificial neural networks (ANN) [3]. However, all these methods permit to determine thermal properties with the presence of significant constraints. A necessity of training a neural network after making any modifications in a model of an object or after making any changes in a range of model's parameters is a very important disadvantage of usage of neural networks. Moreover, application of neural networks requires usage of a set of representative training data.

An alternative approach to solving the problem of thermal properties depth profiling can be usage of genetic (GA) and evolutionary algorithms (EA) [4, 5]. However, the problem was not fully and unequivocally solved, and it remains actual. Application of the GA has significant advantages in relation to usage of ANNs. These are the following: no need for long lasting training, universality, and possibility to use the same method based on the GA for various objects.

2 A method to determine thermal properties

The method to determine thermal properties of layers in a structure is an important extension of the method presented in [5]. It consists of the following stages:

a) Measurements of an amplitude and a phase of a temperature response in areas of a structure (a photoacoustic method with harmonic excitation [6, 7]).
b) Determination of an amplitude (*AC*) and a phase (*PhC*) temperature contrast characteristics [6, 7] in analysed areas of the structure.
c) Thermal modelling of the structure [7].
d) Determination of values of thermal and geometrical parameters for particular layers in examined structure, using the GA.

The main stage of the method is a procedure of fitting theoretical characteristics of the model and measurement characteristics of the examined structure. Matching of these characteristics leads to determination of parameters of the model, which are in the best agreement with properties of the examined object.

3 A thermal model of layered structure

In order to determine the temperature response of an object, a one-dimensional thermal model of layered structure for harmonic excitation was applied [7]. The model is based on an analogy of thermal and electric processes. In the thermal model, a heat flux excited by a source of optical power P is equivalent for current source intensity I, and a temperature response Θ_{front} is equivalent for voltage U. The structure is described in the model with the help of the transmission line matrix TLM [7] and the node matrix of thermal admittances [7].

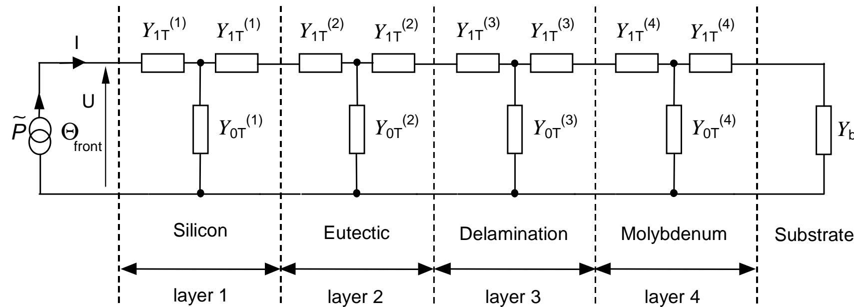

Figure 3.1. One-dimensional TLM–T thermal model of the thyristor structure

Each layer of the structure is represented by TLM-Π or equivalent TLM-T four-terminal network. Series connection of four-terminal networks forms the model of the structure. The one-dimensional TLM–T thermal model of the thyristor structure is presented in fig. 3.1.

In computations, it is possible to apply algorithms well known from theory of electrical circuits. The temperature response Θ_{front} for harmonic excitation with detection of the temperature on the front surface of the structure of n layers can be determined using the following equations [7]:

$$\Theta_{front} = \tilde{P} Z_{in}^{(1,2,\ldots,n)} \qquad Z_{in}^{(i)} = z_{11}^{(i)} - \frac{\left(z_{12}^{(i)}\right)^2}{z_{11}^{(i)} + Z_{in}^{(i+1)}} \tag{1}$$

where $\tilde{P}$ – power of harmonic energetic excitation (complex value), n – number of layers in the structure, i – layer number, $Z_{in}^{(i)}$ – input thermal impedance of layer i, which is loaded by thermal impedance of the next layer $i+1$. In equations (1), for the last thermally thick substrate layer, it is assumed that $Z_{in}^{(n)} = Z_C^{(n)}$. Values of elements $z_{11}^{(i)}$ and $z_{12}^{(i)}$ of impedance matrix of Z-type are described by formulas (2).

$$z_{11}^{(i)} = Z_C^{(i)} \frac{\cosh \Gamma^{(i)}}{\sinh \Gamma^{(i)}} \qquad z_{12}^{(i)} = Z_C^{(i)} \frac{1}{\sinh \Gamma^{(i)}} \tag{2}$$

Characteristic impedance Z_C and operator of propagation Γ are described by equations (3), where i – layer number, ε – thermal effusivity, α – thermal diffusivity, d – thickness of a layer, S – area of excitation, ω – angular frequency.

$$Z_C^{(i)} = (1-j)\frac{1}{S\varepsilon^{(i)}\sqrt{2\omega}} \qquad \Gamma^{(i)} = (1+j)\sqrt{\frac{\omega}{2\alpha^{(i)}}}\, d^{(i)} \tag{3}$$

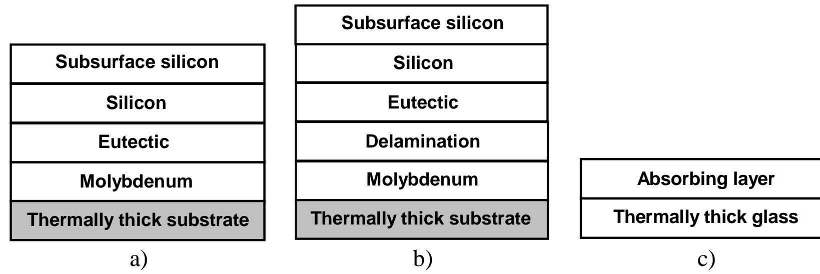

Figure 3.2. Analysed models of objects: a) area of the thyristor structure of good quality of thermocompression, b) delamination area of the thyristor structure, c) external reference object

Models of the thyristor structure for an area of good quality of thermocompression ("*normal*" area, fig. 3.2a), a delamination (fig. 3.2b) and a model of a reference area placed on an external object (fig. 3.2c) were considered.

4 Application of the GA

4.1 Representation of layered structure in the GA

Layered structure is represented by the one-dimensional thermal model. As a result of analysis of the model and taking into consideration features of propagation of thermal waves in layered structure, the following independent variables for each layer were defined: a quotient of thickness and square root of thermal diffusivity $d_i\alpha_i^{-0.5}$ (*dpa*$_i$), a quotient of thermal effusivity of adherent layers $\varepsilon_{i+1}/\varepsilon_i$ (*eps*$_{i+1,\,i}$). A quotient of surface absorption of optical radiation coefficients for surface layers of the examined structure and the reference object β_1/β_{ref} (β_{rel}) was defined. A quotient of effusivities of surface layers of the examined structure and the reference object $\varepsilon_1/\varepsilon_{ref}$ was also defined. Finally, number of independent variables equals $2n+2$ (where n is number of layers).

4.2 Coding of independent variables in a chromosome

The model of the structure, described by independent variables (see p. 4.1) is represented in the GA by a chromosome (fig. 4.1, where n – number of layers).

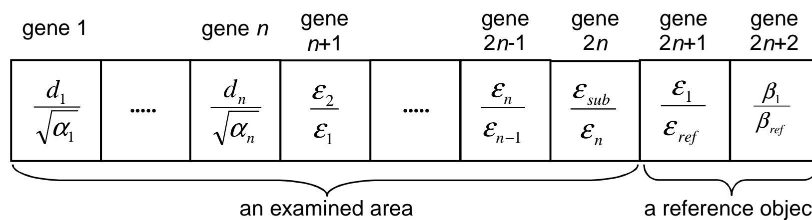

Figure 4.1. General chromosome that represents a thermal model of a structure in the GA

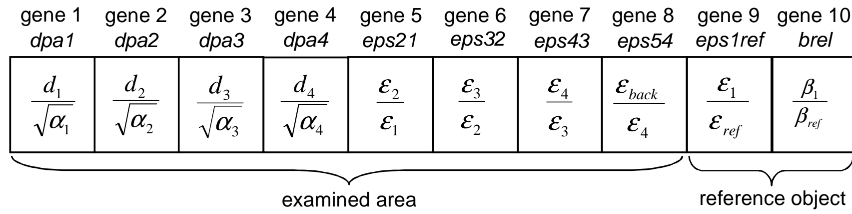

Figure 4.2. Chromosome that represents a thermal model of an example area of the structure

A model of an area of good quality of thermocompression (fig. 3.2a) is described by 10 independent variables (fig. 4.2), and a model of an area of inhomogeneity (fig. 3.2b) is described by 12 variables. A real number representation of genes was applied (so called genetic algorithm with floating point representation).

4.3 An objective function

The objective function F was defined as a sum of normalized mean square errors between characteristic of the model and measured characteristic of the examined object for particular frequencies of harmonic excitation. The function F is described by equation (4), where i – layer number, k – index of frequency of excitation, N – number of frequencies, δ_{AC}, δ_{PhC} – normalised values of mean square errors for amplitude (5a) and phase (5b) contrast characteristics.

$$F = f\left(\frac{d_i}{\sqrt{\alpha_i}}, \frac{\varepsilon_{i+1}}{\varepsilon_i}, \frac{\varepsilon_1}{\varepsilon_{ref}}, \frac{\beta_1}{\beta_{ref}}\right) = \delta_{AC} + \delta_{PhC} \tag{4}$$

$$\delta_{AC} = \sqrt{\sum_{k=1}^{N}\left(\frac{AC_{k\,model} - AC_{k\,measur}}{\Delta AC_{measur}}\right)^2} \tag{5a}$$

$$\delta_{PhC} = \sqrt{\sum_{k=1}^{N}\left(\frac{PhC_{k\,model} - PhC_{k\,measur}}{\Delta PhC_{measur}}\right)^2} \tag{5b}$$

Values of errors δ_{AC} and δ_{PhC} are normalized using division by a difference between minimal and maximal values of measured contrast (6a, 6b).

$$\Delta AC_{measur} = AC_{measur\,MAX} - AC_{measur\,MIN} \tag{6a}$$

$$\Delta PhC_{measur} = PhC_{measur\,MAX} - PhC_{measur\,MIN} \tag{6b}$$

Such normalisation permits to compare and sum errors of different order of magnitude. The aim of the GA was to minimize the objective function F (4).

4.4 A structure and parameters of the GA

A flow chart of computations is presented in fig. 4.3. An initial population was created randomly. Non-linear ranking selection [8] with selection thrust coefficient $q = 0.25$ and elitist model [8] was used. Arithmetic crossover [8] with probability $p_c = 0.8$ was used. The crossover consisted in crossing-over genes that represent the same independent variables. Single-point uniform mutation [8] with probability $p_m = 0.1$ was used. The mutation consisted in random determination of a new value for randomly selected independent variable. The size of population was $n_{pop} = 100$ chromosomes, and the number of generations (iterations of the GA) was 500.

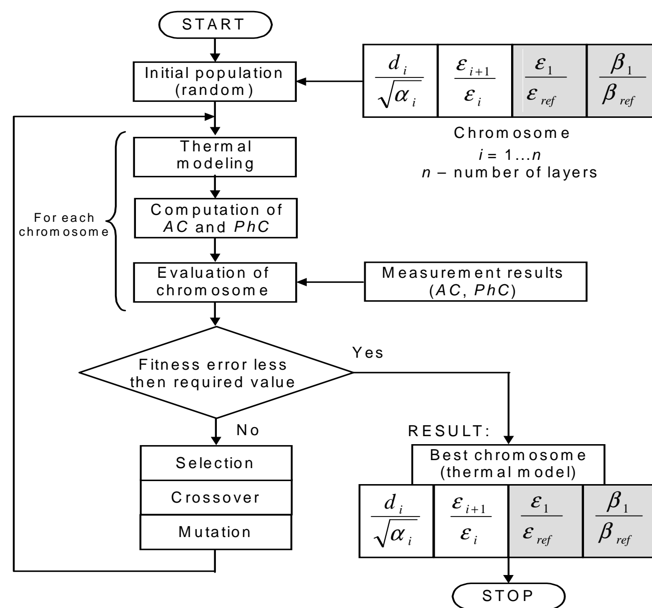

Figure 4.3. Flow chart of computations

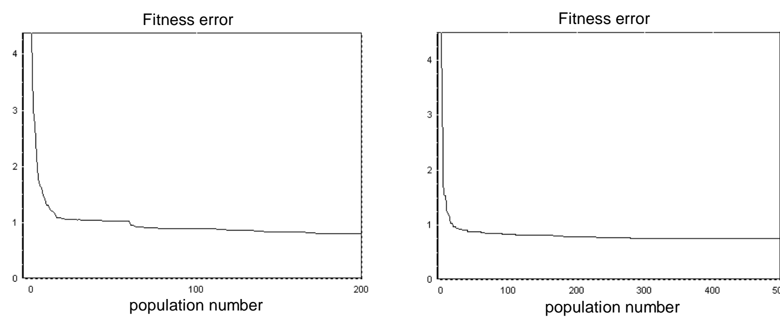

Figure 4.4. Convergence of the GA in example runs of the algorithm

Computations were repeated 100 times for each examined area of the structure, in order to eliminate convergence of the GA to a relative extremum. Values of independent variables averaged for 10% of the best results were taken as a result. Parameters of the GA were chosen experimentally basing on observation of the GA convergence (fig. 4.4).

4.5 Input data

Thermal wave images of the thyristor structure for different frequencies of excitation (fig. 4.5) were acquired using a photoacoustic microscope [6, 7]. Areas of prospective defects *D1*, *D2*, *D3* (fig. 4.6) were chosen for detailed analysis. Several areas of very small contrast (close to zero) in relation to the background (”*normal*” areas *N*, *N1*) were chosen as well. In all these areas, values of the amplitude and the phase of the temperature response were averaged in order to minimize an influence of random measurement errors.

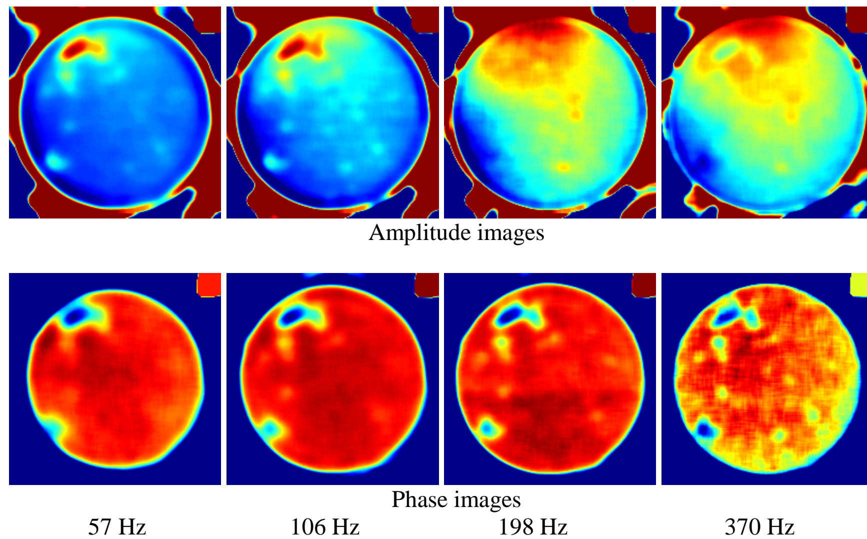

Figure 4.5. Images of examined thyristor structure

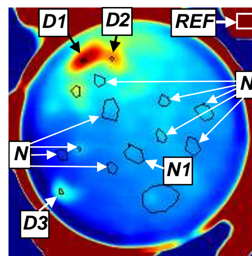

Figure 4.6. Analysed areas of the thyristor structure

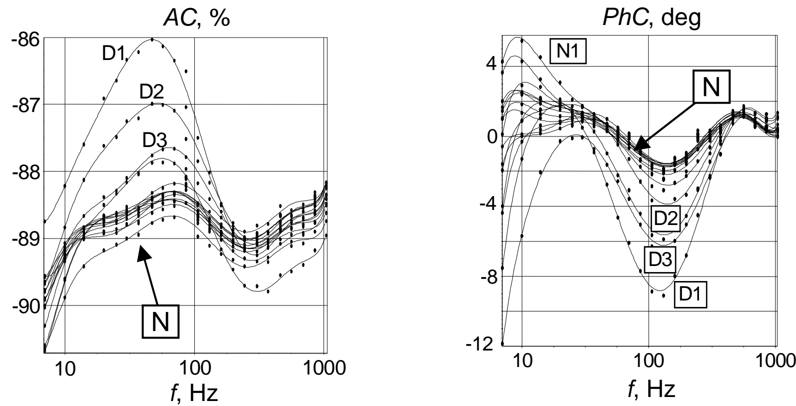

Figure 4.7. Temperature contrast characteristics: the amplitude contrast *AC* and the phase contrast *PhC*

Next, characteristics of the amplitude (*AC*) and the phase (*PhC*) temperature contrast in frequency domain were determined for each area considered. These characteristics (fig. 4.7) are the input data for the GA.

5 Results

5.1 Parameters chosen for computations

Values of thermal properties of materials [7, 9] were chosen for computations (table 5.1). These properties were the following: thermal conductivity λ, density of material ρ, specific heat c. They were used to determine thermal diffusivity α and thermal effusivity ε using formulas (7).

$$\alpha = \frac{\lambda}{\rho\ c} \qquad \varepsilon = \sqrt{\lambda \rho\ c} \tag{7}$$

Next, boundary values of parameters of particular layers in the thyristor structure were computed (table 5.2). Thickness' of layers *d* were assumed according to the data taken from the manufacturer, with a certain tolerance.

Table 5.1. Nominal values of thermal properties of materials

Material	λ $W{\cdot}m^{-1}{\cdot}K^{-1}$	ρ $kg{\cdot}m^{-3}$	c $J{\cdot}kg^{-1}{\cdot}K^{-1}$	$\alpha \cdot 10^{-6}$ $m^2{\cdot}s^{-1}$	ε $W{\cdot}s^{0.5}{\cdot}m^{-2}{\cdot}K^{-1}$
silicon (Si) average	125	2330	678	80.0	14000
aluminium (Al)	237	2700	902.5	97.3	24025
molybdenum (Mo)	138	10250	250.2	53.8	18812
air	0.026	1.205	1005.0	21.4	5.6
glass	1.1	2500	700.0	0.63	1387

Table 5.2. Boundary values of parameters of layers in the thyristor structure

	Layer	$d \cdot 10^{-6}$, m		$\alpha \cdot 10^{-6}$, $m^2 \cdot s^{-1}$		ε, $W \cdot s^{0.5} \cdot m^{-2} \cdot K^{-1}$	
		d_{min}	d_{max}	α_{min}	α_{max}	ε_{min}	ε_{max}
1	silicon (subsurface)	0.001	20	10	120	4000	18000
2	silicon (internal)	300	400	60	120	12000	18000
3	eutectic Si–Al	40	100	10	100	1000	18000
4	delamination (air)	0.01	1	10	100	5	18000
5	molybdenum	1200	1200	30	60	14000	19500

It was assumed, that the reference object (fig. 3.2c) is thermally thick, and effusivity of glass is 1200÷1500 $W \cdot s^{0.5} \cdot m^{-2} \cdot K^{-1}$. Using data from table 5.2, boundary values of variables dpa_i ($d_i\alpha_i^{-0.5}$) and $eps_{i+1,\,i}$ ($\varepsilon_{i+1}/\varepsilon_i$) were computed using equations (8a) and (8b).

$$\frac{d_i}{\sqrt{\alpha_i}} \in \left\langle \frac{d_{i\,\min}}{\sqrt{\alpha_{i\,\max}}}, \frac{d_{i\,\max}}{\sqrt{\alpha_{i\,\min}}} \right\rangle \tag{8a}$$

$$\frac{\varepsilon_{i+1}}{\varepsilon_i} \in \left\langle \frac{\varepsilon_{i+1\,\min}}{\varepsilon_{i\,\max}}, \frac{\varepsilon_{i+1\,\max}}{\varepsilon_{i\,\min}} \right\rangle \qquad \frac{\varepsilon_1}{\varepsilon_{ref}} \in \left\langle \frac{\varepsilon_{1\,\min}}{\varepsilon_{ref\,\max}}, \frac{\varepsilon_{1\,\max}}{\varepsilon_{ref\,\min}} \right\rangle \tag{8b}$$

The quotient of optical radiation absorption coefficients $\beta_{rel} \in <0, 10>$ was assumed.

5.2 Analysis of thermal properties

Obtained results of the fitting procedure for characteristics of the model (solid line) and measured characteristics for *D1* area (fig. 4.6) are presented in fig. 5.1. A method for determination of parameters of layers in the thyristor structure (fig. 5.2) will be demonstrated using an example model of four-layer structure that represents "*normal*" area *N1* (fig. 3.2a) and using an example model of five-layer structure that represents areas of defects *D1*, *D2*, *D3* (fig. 3.2b).

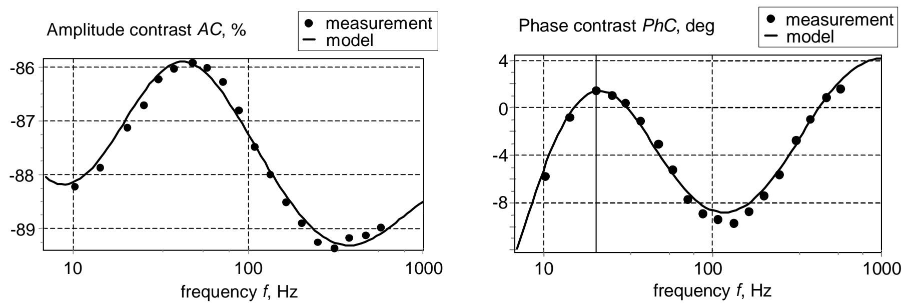

Figure 5.1. Results of the fitting procedure for *D1* area

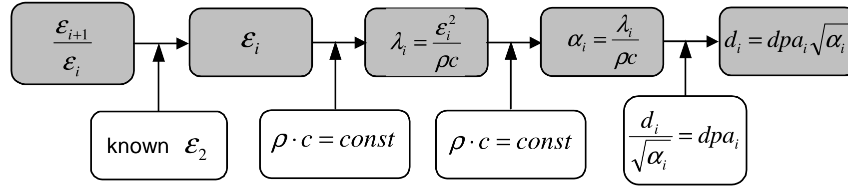

Figure 5.2. **Algorithm for computation of parameters of layers**

It was assumed, that thermal effusivity ε is the quantity for determination of other properties. It was also assumed, that thermal effusivity of silicon is known (ε_2 = 14000 $Ws^{0.5}m^{-2}K^{-1}$). Thermal effusivities of other layers were computed basing on quotients $\varepsilon_{i+1}/\varepsilon_i$ using formulas (9b).

$$\varepsilon_i = \frac{\varepsilon_{i+1}}{eps_{i+1,\,i}} \tag{9a}$$

$$\varepsilon_2 = \varepsilon_1 eps21 \qquad \varepsilon_3 = \varepsilon_2 eps32 \qquad \varepsilon_4 = \varepsilon_3 eps43 \tag{9b}$$

For silicon and molybdenum layers, it was assumed, that thermal capacity C_{th} = ρc is constant and known. For these layers, computations were performed using the procedure shown in fig. 5.2. Unfortunately, condition $C_{th} = const$ is not satisfied for delamination and eutectic. Therefore, it is not possible to determine other parameters of these layers except thermal effusivity ε. Using the procedure in fig. 5.2 and basing on values of independent variables determined by the GA, parameters of layers of the thyristor structure (table 5.3) were computed in considered areas (fig. 4.6).

Table 5.3. Averaging values of parameters of selected areas in the structure

Layer	Thermal effusivity ε $W \cdot s^{0.5} \cdot m^{-2} \cdot K^{-1}$				Thermal conductivity λ $W \cdot m^{-1} \cdot K^{-1}$			
	D1	*D2*	*D3*	*N1*	*D1*	*D2*	*D3*	*N1*
silicon subsurface	7952	8623	7442	8017	43.0	51.1	37.4	45.0
silicon internal	14000	14000	14000	14000	124.1	124.1	124.1	124.1
eutectic Si–Al	5895	6903	6742	4988				
delamination	77	74	79					
molybdenum	15203	16040	13793	**15109**	90.1	100.3	74.2	89.0

Layer	Thermal diffusivity $\alpha \cdot 10^{-6}$ $m^2 \cdot s^{-1}$				Thickness *d* μm			
	D1	*D2*	*D3*	*N1*	*D1*	*D2*	*D3*	*N1*
silicon (subsurface)	27.2	32.4	23.7	28.5	9	7	4	6
silicon (internal)	78.5	78.5	78.5	78.5	307	326	313	395
molybdenum	35.1	39.1	28.9	34.7				

Basing on values of thermal effusivities ε (table 5.3), a reflection ratio of the thermal wave between particular layers was computed. The reflection ratio of the thermal

wave r_{21} between a layer 1 and a layer 2 can be defined using equation (10), where ε_1 and ε_2 are thermal effusivities of adjacent layers.

$$r_{21} = \frac{|\varepsilon_1 - \varepsilon_2|}{\varepsilon_1 + \varepsilon_2} = \frac{\left|1 - \frac{\varepsilon_2}{\varepsilon_1}\right|}{1 + \frac{\varepsilon_2}{\varepsilon_1}} \tag{10}$$

The value $r = 1$ indicates that total reflection of the thermal wave takes place. Obtained results (table 5.4) confirm that internal defects exist in examined thyristor structure between eutectic and molybdenum layers. Values of the reflection ratio close to 1 indicate that these defects are probably voids or delaminations.

Table 5.4. Averaging values of the reflection ratio of the thermal wave

	Interface	Reflection ratio of the thermal wave r			
		D1	*D2*	*D3*	*N1*
r_{21}	subsurface–internal silicon	0.29	0.24	0.32	0.29
r_{32}	internal silicon–eutectic	0.46	0.44	0.47	0.48
r_{43}	eutectic–delamination	0.95	0.96	0.95	0.51
r_{54}	delamination–molybdenum	0.99	0.99	0.99	
r_{65}	molybdenum–substrate	0.97	0.74	0.97	0.57

The most important conclusions from analysis of obtained results are the following:

a) There is a subsurface layer of silicon in the thyristor structure (thickness d 4÷9 μm) of worse thermal properties than internal silicon.
b) It was confirmed, that thermal effusivity ε of silicon–aluminium eutectic is smaller than both silicon and aluminium effusivity.
c) Very small effusivity of a layer between eutectic and molybdenum indicates, that this layer is delamination or highly non-uniform eutectic with defects.
d) It was found, that effusivity ε of molybdenum is smaller than typical value for this metal (thermal conductivity λ is 1.5 times smaller than the nominal).

The value of thermal effusivity of internal silicon ε_2 was taken as a radix value to determine effusivities of other layers and to compute other properties. Therefore, it should be underlined, that in the method proposed, it is very important to properly measure and assume thermal effusivity of silicon.

In order to verify obtained results destructive investigations of the thyristor structure were performed. Imaging areas *D1, D2, D3* using a scanning electron microscope showed that these areas are delaminations.

6 Conclusions

The new method of determination of thermal properties depth profile in layered structures was presented. The method is based on fitting theoretical characteristics of the thermal model and measured characteristics of the examined object. The procedure of fitting is performed using the GA. Obtained results permit to analyse thermal properties of each layer in detail. The method can be applied for investigation of thermal properties of various layered structures.

References

1. Laurics W., Glorieux C., Thoen J., (1991). Depth profiling by Fourier analysis of photoacoustic signals, *Physical Acoustics, Fundamentals, and Applications*, New York, Plenum Press, pp. 433–436.
2. Li Voti R., Liakhou G.L., Paoloni S., Sibilia C., Bertolotti M., (2001). Photothermal depth profiling by thermal wave backscattering theory, *Analytical Sciences*, Vol. 17, No. 12, 2001, p. 414.
3. Glorieux C., Thoen J., (1996). Thermal depth profile reconstruction by neural network recognition of the photothermal frequency spectrum, *Journal of Applied Physics*, Vol. 80, No. 11, 1996, pp. 6510–6515.
4. Li Voti R., et all, (2001). Use of the genetic algorithm in the photothermal depth profiling, *Analytical Sciences*, Vol. 17, No. 12, 2001, p. 410.
5. Arsoba R., Suszyński Z., (2004). Application of photoacoustic method and evolutionary algorithm for determination of thermal properties of layered structure, *Journal de Physique IV*, Vol. 117, 2004, pp. 1–6.
6. Arsoba R., (2006). *Badanie jakości termokompresji w strukturach tyrystorowych metodami termofalowymi dla pobudzeń energetycznych zmiennych w czasie lub przestrzeni* (in Polish), Ph.D. Thesis, Koszalin University of Technology, Poland.
7. Suszyński Z., (2001). *Termofalowe metody badania materiałów i przyrządów elektronicznych* (in Polish), Koszalin, Wydawnictwo Politechniki Koszalińskiej.
8. Michalewicz Z., (1996). *Genetic algorithms + data structures = evolution programs*, Berlin Heidelberg, Springer–Verlag.
9. Bodzenta J., (1999). *Fale termiczne w badaniach ciał stałych* (in Polish), Zeszyty Naukowe Politechniki Śląskiej, Gliwice, Matematyka–Fizyka, wolumen 85.